Supporting Information for "How frequent are Antarctic sudden stratospheric warmings in present and future climate?"

DOI: 10.1002/2021GL093215

M. Jucker[1,2], T. Reichler[3], and D. W. Waugh[4,5]

[1]Climate Change Research Centre, The University of New South Wales, Sydney, NSW, Australia

[2]Australian Research Council Centre of Excellence for Climate Extremes, Sydney, NSW, Australia

[3]Department of Atmospheric Sciences, University of Utah, Salt Lake City, UT, USA

[4]Department of Earth and Planetary Sciences, The Johns Hopkins University, Baltimore, MD, USA

[5]School of Mathematics and Statistics, The University of New South Wales, Sydney, NSW, Australia

Contents of this file

1. Text S1 to S6
2. Figures S1 to S3
3. Table S1

Text S1. CM2.1 validation In addition to the discussion in the main text, Fig. S1 shows the latitude-pressure zonal mean zonal wind seasonal climatologies of the mean and interannual standard deviation. The model shows good agreement at all levels and seasons, although there is some overestimation of southern upper stratospheric variability in September-October-November and the model does not simulate the Quasi-Biennial Oscillation, resulting in underestimates in tropical interannual variability.

Text S2. The 2002 and 2019 events Fig. S2 shows the evolution of u_{1060} and polar cap stratospheric ozone during the springs of 2002 and 2019 from ERA5.

Text S3. Surface impacts Just as for the observed SSWs, in our present-day simulation SSWs are followed by a negative phase of the SAM on a monthly to seasonal timescale (Fig. S3a; only composites for SSW-weak are shown) (Thompson et al., 2005), accompanied by colder and wetter conditions over New Zealand and South America as well as warmer and drier conditions over Eastern Australia (Figs. S3b and S3c). These surface impacts agree well with previous work (Gillett et al., 2006; Lewis, 2019; Lim et al., 2019) and the reanalysis data from the 2002 and 2019 events, confirming that our model reproduces the dynamical evolution of SSWs well and that our definition based on anomalous u_{1060} does indeed capture events with considerable surface impact. We note that the surface impact of early SSW-weak events (e.g. those occurring in June and July) is similar to the impact of later events (not shown).

Text S4. CMIP6 model selection We consider pre-industrial control (piControl) and Shared Socioeconomic Pathway 585 (SSP585) (O'Neill et al., 2014) simulations (which include e.g. ozone hole recovery, Fig. 4 and Table S1). The models from the CMIP6 archive were chosen based on the availability of daily data for both piControl and SSP585 scenarios, and given the lack of stratospheric variability in low top models (Charlton-Perez et al., 2013), we require a well resolved stratosphere with at least 30 vertical levels and a model top at or above 1 hPa. For piControl we required at least 100 years of data for sufficient statistics. The five models that fulfill all these conditions are CESM2-WACCM, CanESM5, GFDL-CM4, INM-CM5-0, MIROC6, and the data used comprise a total of 3,341 years of piControl as well as 5x80 years of SSP585 (from 2021 to 2100). One ensemble member (r1i1p1f) for each model was considered.

Text S5. Uncertainty estimates For the two CM2.1 simulations, frequency uncertainties in Fig. 2 are computed by splitting the 9,900 years (after 90 years spinup) into 99 century-long non-overlapping segments, and computing the mean and standard deviation from this ensemble. For CMIP6 there are not enough events for similar statistical calculations, and the raw results are reported in Table S1.

Text S6. Return time If SSWs are random and independent, we should be able to model them as a Poisson process. For such a process, the return or waiting time can be computed using an exponential distribution with an expectation value equal to the mean occurrence frequency: PDF = $\lambda \exp(-\lambda x)$, where λ is the average frequency (e.g. 1/21.6 years for present-day SH SSW-weak events) and x is the waiting time in years (Gumbel, 1941). This is an approximation to a binomial distribution assuming large sample size and low probability. Since in our case we do not always have large sample size, we compute the return time using the binomial distribution. Then, the return time distribution is determined by the probability of zero events during a given time period ($k = 0$, $n =$number of years, $p = 1/$mean return time to be fitted). This has the advantage of being able to compute the probabilities for an arbitrary number of events, while still being able to check the validity of randomness and independence. The cumulative distribution function of the exponential distribution is an approximation (again large sample size and low probability) for the survival function of a binomial distribution for zero events. Therefore, we use the latter to compute the probability of one or more events within a given time period, provided the events are independent and random.

Explicitly, the return time PDF of a random and independent process follows a binomial distribution of zero events, as the return time corresponds to the probability of no event happening within a given time interval:

$$P(y) = \left[\sum_{k=0}^{k=N} \binom{y}{k} \left(\frac{1}{\tau}\right)^k \left(1 - \frac{1}{\tau}\right)^{y-k} \right]_{N=0} = \left(1 - \frac{1}{\tau}\right)^y, \tag{1}$$

where y is the time interval in years, $N(=0)$ is the number of events, and τ is the mean time interval between two SSWs (e.g. 21.6 years for present-day SSW-weak events). This is what is shown as solid black line in the return time plots of Fig. 2.

The probability of one or more events within a given time interval is simply $1 - P(y)$, which is shown as dashed black line in the return time plots. This so-called 'survival function' is used along with the cumulative probability function (as shown above but not setting $N = 0$) and the mass probability function (without the summation) to compute the various probabilities reported in the text and Table **??**. For instance, the probability of at least one SSW-reversal in 80 years is $1 - (1 - 1/883)^{80} \approx 8.7\%$, and the probability of exactly two SSW-weak events in 41 years of present-day conditions is

$$\binom{41}{2} \left(\frac{1}{21.6}\right)^2 \left(1 - \frac{1}{21.6}\right)^{41-2} \approx 28\%, \tag{2}$$

as reported in Table 1.

References

Charlton-Perez, A. J., Baldwin, M. P., Birner, T., Black, R. X., Butler, A. H., Calvo, N., … Watanabe, S. (2013). On the lack of stratospheric dynamical variability in low-top versions of the CMIP5 models. *Journal of Geophysical Research Atmospheres*, *118*(6), 2494–2505. doi: 10.1002/jgrd.50125

Gillett, N. P., Kell, T. D., & Jones, P. D. (2006). Regional climate impacts of the Southern Annular Mode. *Geophysical Research Letters*, *33*(23), 1–4. doi: 10.1029/2006GL027721

Gumbel, E. J. (1941). The Return Period of Flood Flows Author (s): E . J . Gumbel Source : The Annals of Mathematical Statistics , Vol . 12 , No . 2 (Jun ., 1941), pp . 163-190 Published by : Institute of Mathematical Statistics Stable URL : http://www.jstor.org/stable/223. *The Annals of Mathematical Statistics*, *12*(2), 163–190. Retrieved from https://www.jstor.org/stable/2235766

Lewis, D. (2019, 10). Rare warming over Antarctica reveals power of stratospheric models. *Nature*, *574*(7777), 160–161. Retrieved from http://www.nature.com/articles/d41586-019-02985-8 doi: 10.1038/d41586-019-02985-8

Lim, E.-P., Hendon, H. H., Boschat, G., Hudson, D., Thompson, D. W. J., Dowdy, A. J., & Arblaster, J. M. (2019, 11). Australian hot and dry extremes induced by weakenings of the stratospheric polar vortex. *Nature Geoscience*, *12*(11), 896–901. Retrieved from http://dx.doi.org/10.1038/s41561-019-0456-xhttp://www.nature.com/articles/s41561-019-0456-x doi: 10.1038/s41561-019-0456-x

O'Neill, B. C., Kriegler, E., Riahi, K., Ebi, K. L., Hallegatte, S., Carter, T. R., … van Vuuren, D. P. (2014). A new scenario framework for climate change research: The concept of shared socioeconomic pathways. *Climatic Change*, *122*(3), 387–400. doi: 10.1007/s10584-013-0905-2

Thompson, D. W. J., Baldwin, M. P., & Solomon, S. (2005, 3). Stratosphere–Troposphere Coupling in the Southern Hemisphere. *Journal of the Atmospheric Sciences*, *62*(3), 708–715. Retrieved from `http://journals.ametsoc.org/doi/abs/10.1175/JAS-3321.1` doi: 10.1175/JAS-3321.1

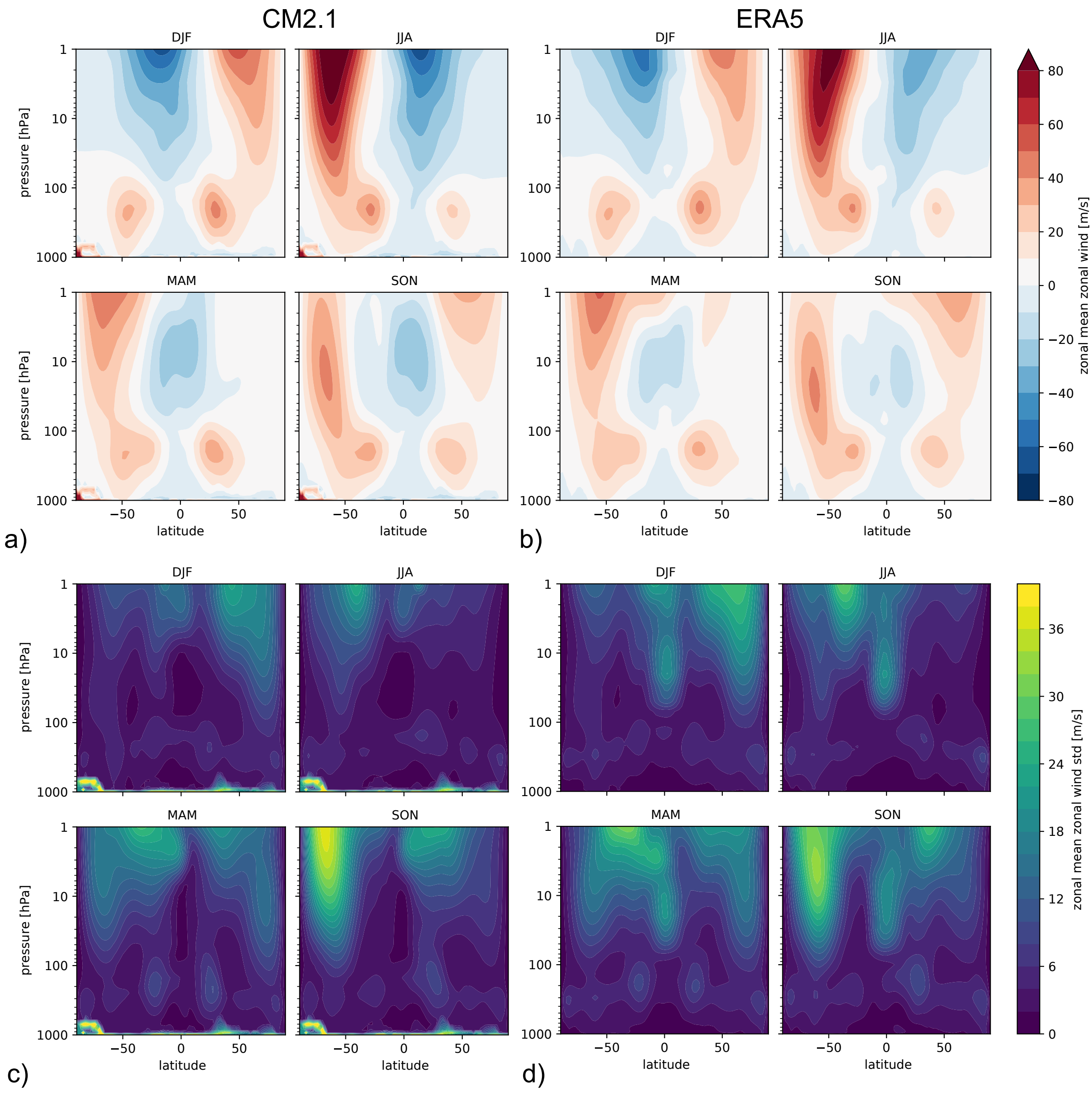

Figure S1. Comparison of (left) CM2.1 and (right) ERA5 zonal mean zonal wind climatology (a,b) and interannual standard deviation (c,d).

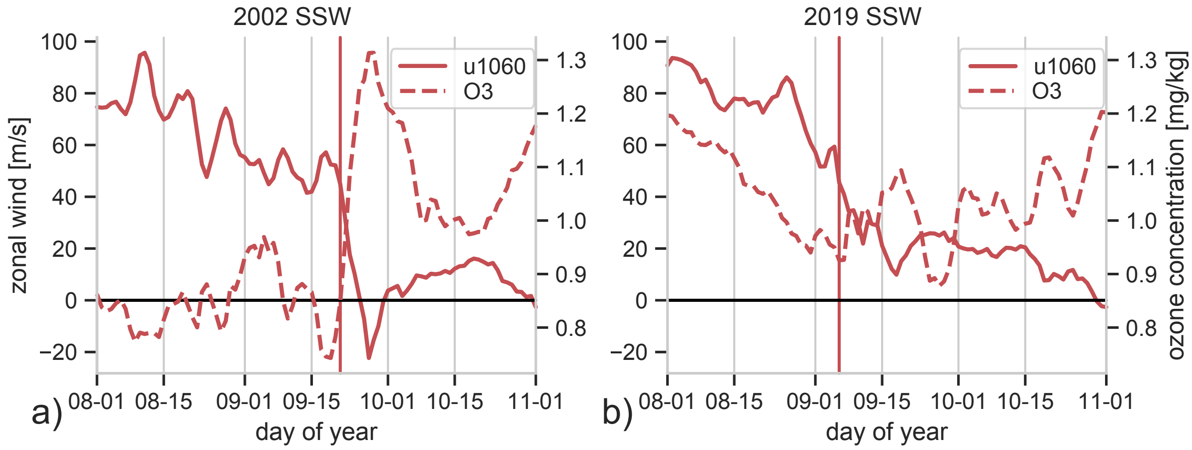

Figure S2. u_{1060} (solid), and polar cap (60-90°S) averaged ozone mass mixing ratio at 50 hPa (dashed) for the springs of (a) 2002 and (b) 2019 from ERA5 reanalysis. The solid vertical lines denote the onset date based on the SSW-weak definition.

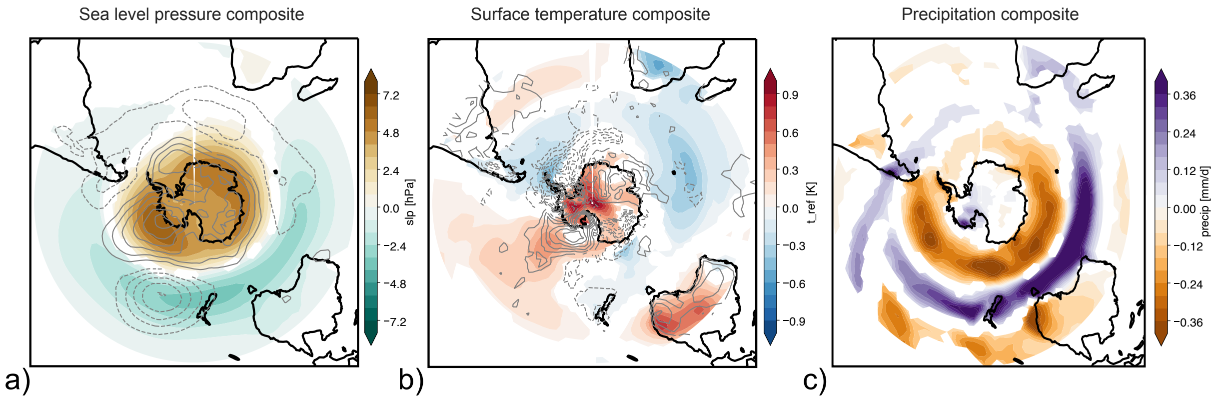

Figure S3. Composited surface anomalies averaged 0-60 days after the onset day for (a) surface pressure, (b) surface temperature and (c) precipitation for present-day CM2.1 SSW-weak events. The composites of the 2002 and 2019 events from ERA5 are added in gray contours for direct comparison except for precipitation which is too noisy in ERA5. Anomalies are relative to daily climatology, and only values which are statistically significant at the 5% level (two-sided *t*-test) are plotted.

Model	# years	# SSW-weak	mean return time [years]	# SSW-weak per 80 years	# SSW-weak 2021-2100
CESM2-WACCM	500	15	33.3	2.40	0
CanESM5	1000	6	166.7	0.48	1
GFDL-CM4	140	1	140.0	0.57	1
INM-CM5-0	1201	5	240.2	0.33	0
MIROC6	500	5	100.0	0.80	1

Table S1. Statistical information for CMIP6 data. All columns except the last refer to piControl simulations, whereas the last reports results from the SSP585 simulations. The second last column normalizes the number of SSW-weak events in piControl to a 80-year period for direct comparison to 2021-2100. All models except CESM2-WACCM strongly underestimate the number of SSWs, and no model produces more than one single event between 2021 and 2100.